DOI: 10.1002/ejic.200800772

Sulfoxygenation Catalysed by Oxidovanadium Complexes

Pingsong Wu,[a] Cem Çelik,[a] Gabriella Santoni,[a] Jérome Dallery,[a] and Dieter Rehder*[a]

Keywords: Oxidovanadium complexes / Ethanolamines / Sulfoxygenation / Models of peroxidases / Vanadate-dependent peroxidase

Model complexes of vanadate-dependent peroxidases, viz. oxidovanadium(V) complexes of the general composition $[VO(H_{n-x}L)]$, have been prepared and characterised. H_nL is an n-basic di- or trichiral aminodiethanol $[HOCH(Ph)-CH_2]_2NR$, with R = *N*-methylimidazolyl (H_2L^A), tris(hydroxymethyl)methyl (H_5L^B, 2 isomers), 2,3-dihydroxypropyl (H_4L^C, 2 isomers) and 2-hydroxy-3-trityloxypropyl (H_3L^D). These ligands form the complexes $[VO(OH)(L^A)]$, $[VO(H_2L^B)]$, trigonal-bipyramidal $[VO(HL^C)]_{tbp}$ and octahedral Λ-$[VO(HL^C)]_{oct}$. The ligands *R*,*R*,*S*-H_4L^C and *R*,*R*,*R*-H_3L^D, and the complexes Λ-$[VO(R,R,S\text{-}HL^C)]_{oct}$ and $[VO(R,R,S\text{-}HL^C)]_{tbp}$ have been characterised by X-ray structure analysis. The complexes $[VO(H_2L^B)]$ and $[VO(HL^C)]$ were immobilised on Merrifield and Barlos resin by anchoring through a free alcoholic group in the ligand side-chain R. $\{[VO(H_2O)L^E]\}$, an oxidovanadium(IV) complex tethered to Merrifield resin, was prepared by treating $[VO(acac)_2]$ with $\{HL^E\}$, the immobilised Schiff base ligand obtained by condensation of salicylaldehyde with resin-anchored lysine. The complexes and in situ systems ($[VO(O\textit{i}Pr)_3]$ + ligand) as well as the immobilised complexes were investigated for their catalytic activity in the oxygenation, by cumyl hydroperoxide, of thioanisol to its sulfoxide. All of the systems were active, with a selectivity (sulfoxide vs. sulfone) of 95–98 %. Satisfactory turnover rates and a chiral induction up to 37 % *ee* were observed.

Introduction

Chiral sulfoxides are important synthons in organic chemistry, in particular for enantioselective carbon-carbon bond formation. The general importance of sulfoxides in inorganic synthesis and in medication, and approaches to their stereoselective synthesis have recently been surveyed.[1] In addition, sulfoxides play a critical role in biological activity, e.g. in the formation of dimethyl sulfoxide from dimethyl sulfide as the initiating step in the oxidative conversion of organic sulfur (such as dimethyl sulfide and thiophene) to inorganic sulfur compounds. Several enzymes are able to catalyse the oxygenation of sulfides to sulfoxides. Examples are ammonia monooxygenase from *Nitrosomonas europae*,[2a] bacterial cyclohexane monooxygenases[2b] and dioxygenase from *Pseudomonas putida*.[3] Haloperoxidases isolated from a variety of marine macro-algae such as the sea weed *Ascophyllum nodosum* are also capable of catalysing sulfoxygenations.[4,5] These enzymes contain vanadate $[H_2VO_4]^-$ in their active centre linked to a histidine of the protein matrix.[6] Vanadium is in a trigonal-bipyramidal environment, with the histidine Nε and a hydroxo group in the apical positions. In these enzymes, vanadium(V) does not function by switching between different oxidation states (as commonly observed in oxidation reactions catalysed by vanadium compounds[7]) but as a Lewis acid through activation, by coordination, of peroxide. The genuine reaction catalysed by these enzymes is the two-electron oxidation of halide by hydrogen peroxide to, e.g., hypohalous acid [Equation (1), upper trace], a reaction which consumes protons.[8] Similarly, sulfides can be oxygenated to sulfones [Equation (1), lower trace] and the reaction is usually enantioselective if prochiral sulfides are employed. Protons are not consumed in sulfoxygenation but they are, however,

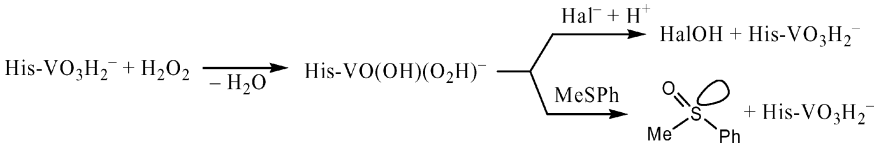

(1)

necessary as cocatalysts. The reaction path has been evaluated by DFT calculations, according to which the rate-limiting step in the oxygenation of sulfide to sulfoxide is the

[a] Chemistry Department, University of Hamburg, 20146 Hamburg, Germany
E-mail: rehder@chemie.uni-hamburg.de

simultaneous formation of the S–O bond and breaking of the peroxo O–O bond.[9]

Stimulated by the potential of algal peroxidases in sulfoxygenation, model reactions were developed in which vanadium-based catalysts were employed to (enantioselectively) oxidise sulfides,[10–12] disulfides,[12a,13] thioacetals[12a] and thianthrene[14] to the respective sulfoxides, using H_2O_2, organic peroxides or peroxo acids as oxidants. The catalysts typically employed are in situ systems consisting of $[VO(acac)_2]$ [acac = acetylacetonate(1–)] or $[VO(OR')_3]$ (R′ = *i*Pr, *t*Bu) as the vanadium component and a chiral trifunctional Schiff base ligand, or preformed vanadium (pre)-catalysts such as $[VO(O_2)heida]^-$ [H_2heida = *N*-(2-hydroxyethyl)iminodiacetic acid].[15]

Our approach to enzyme models has been the design of vanadium complexes mimicking the coordination environment of vanadate-dependent haloperoxidases with respect to both the nature of the donor set and the coordination geometry. These structural and functional mimics are represented by oxidovanadium(V) complexes formed with chiral ligands derived from tridentate diethanolamines $(HOCH(Ph)CH_2)_2NR$, H_2L.[16–19] The present work is an extension to ligands additionally functionalised in the side-chain represented by R, providing a more rigid coordination sphere for VO^{3+} and the possibility of anchoring the vanadium site to a solid substrate, Merrifield and Barlos resins in this case.

Results and Discussion

Characterisation of Ligands and Complexes

Scheme 1 provides an overview of ligands and complexes which have been characterised and used in homogeneous catalysis in the present study. The ligands are derived from dichiral diethanolamines, with an additional functionalised substituent on the amine nitrogen. They are prepared by treating R-styrene oxide with the primary amines H_2NR in a 1:2 molar ratio and subsequent workup by flash-chromatography on silica gel. A racemic amine was employed in the case of R = 1,2-dihydroxypropyl (→ H_4L^C). The main product thus obtained results from the 1,3-cleavage of the epoxide (H_2L^A, H_5L^B and H_4L^C) along with same product from the 1,2-cleavage ($H_5L^{B'}$, $H_4L^{C'}$) and minor amounts of secondary amines. H_3L^D was obtained by treatment of H_4L^C with trityl chloride in the presence of $N(iPr)_2Et$ (Hünig's base). The ligands H_2L^A, H_5L^B, $H_5L^{B'}$, H_4L^C and $H_4L^{C'}$ were identified by their spectroscopic characteristics (see Exp. Section). The trichiral potentially pentadentate H_4L^C and the tetradentate H_3L^D have been structurally characterised by XRD. For selected structure parameters see Table 1, for drawings see Figure 1. An interesting feature in the structure of H_4L^C is the comparatively short distance between N1 and O3 (the β-OH of the propanediol moiety) of 2.82 Å which is less than the sum of

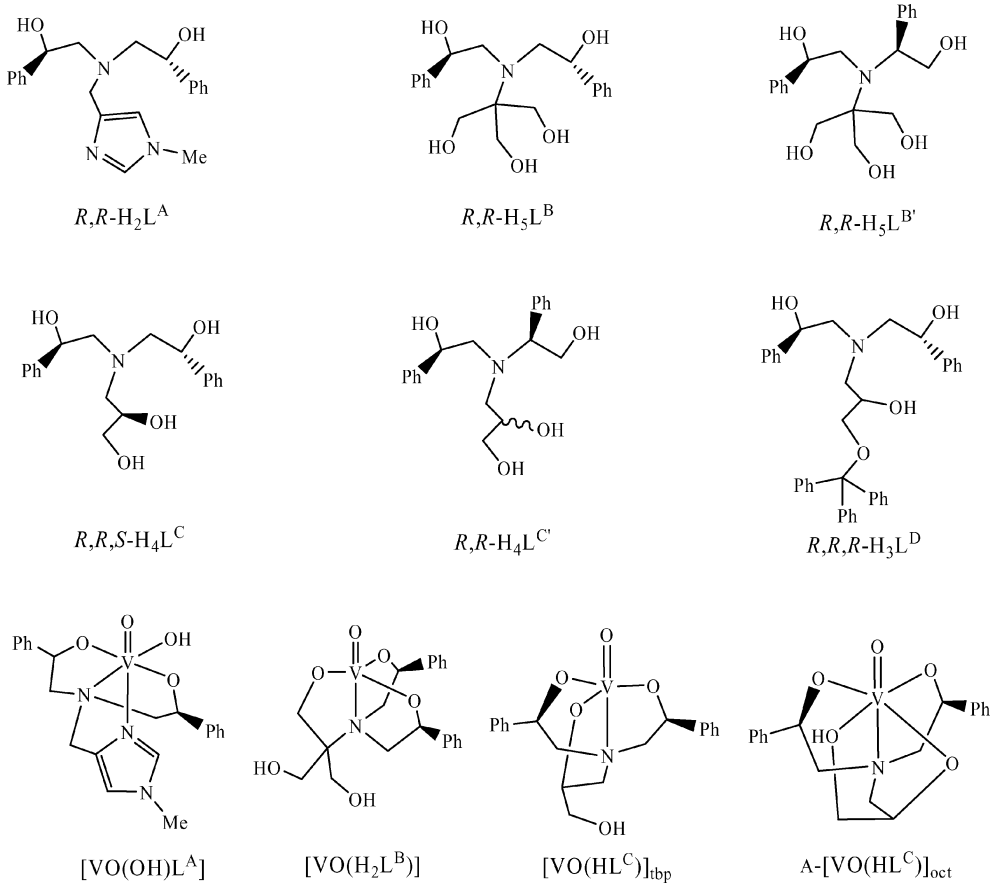

Scheme 1.

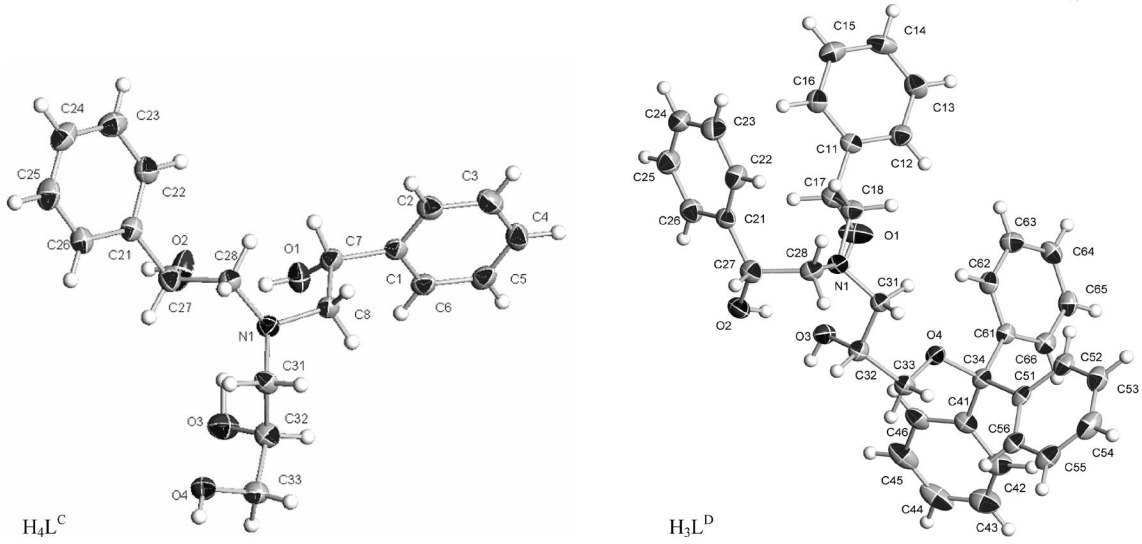

Figure 1. Structure representations of the ligands of H_4L^C and H_3L^D.

the van der Waals radii (3.05 Å). This proximity is induced by "proton sharing" between N1 and O3. The N···H···O angle is 118.5°.

Table 1. Selected bond lengths [Å] and angles [°] for H_4L^C and H_3L^D.[a]

H_4L^C		H_3L^D	
av. *d*(N1–C)	1.464	av. *d*(N1–C)	1.475
C7–O1	1.426(3)	C17–O1	1.441(3)
C27–O2	1.431(3)	C27–O2	1.429(4)
C32–O3	1.420(3)	C32–O3	1.423(3)
C33–O4	1.426(3)	C33–O4	1.425(3)
		C34–O4	1.448(3)
av. N1	113.7	av. N1	114.9
N1–C8–C7	113.68(18)	N1–C18–C17	110.9(3)
N1–C28–C27	111.03(18)	N1–C28–C27	110.0(3)
av. C32	110.1	av. C32	110.8
O4–C33–C32	110.43(18)	O4–C33–C32	107.1(2)
		C33–O4–C34	119.0(2)
(OH)1···O2	2.850	(OH)1···O3	2.778
(OH)2···O4	2.818	(OH)2···O3	3.114
(OH)4···O1	2.866	(OH)3···O2	2.707
		(OH)2···N1	2.721

[a] For one of the two molecules in the asymmetric unit.

As we have shown previously,[16] tridentate aminodiethanols H_2L react with $[VO(OiPr)_3]$ to form the pentacoordinate, somewhat distorted trigonal-bipyramidal complex [VO(O*i*Pr)-L], which converts to [VO(OMe)L] in methanol. Reaction of ligand H_2L^A (containing the imidazolyl substituent) with $[VO(OiPr)_3]$ in THF yields an oxidovanadium(V) complex of the likely composition $[VO(OH)L^A]$, with the octahedral coordination environment proposed in Scheme 1. The imidazole moiety in multidentate ligands can coordinate to or remain uncoordinated from the oxidovanadium unit. An example for the former is the complex $[V^{IV}O(salim)acac]$ (salim is the Schiff base formed between salicylaldehyde and 2-aminoethylimidazole)[20] and an example for the latter is $[V^VO_2(nap\text{-}his)]$ (nap-his is the Schiff base formed from *o*-hydroxynaphthaldehyde and histidine).[21] The main evidence for participation of the aromatic imidazole-N and thus an O_4N_2 donor set is provided by ^1H NMR spectroscopy: the ^1H coordination shift for the C–H proton adjacent to the coordinating N amounts typically to 0.31 ppm.[22] The ^{51}V NMR spectrum of a solution of $[VO(OH)L^A]$ in CD_2Cl_2 shows two signals at –495 and –501 ppm (integral intensities 1:0.7) which are clearly to high field, by 30–60 ppm, of the $\delta(^{51}V)$ shift of the trigonal-bipyramidal oxidovanadium complexes containing an O_4N donor set.[16,18] Such a high-field shift is expected on going from penta- to hexacoordination.[23] The presence of two signals reflects the presence of two isomers. Addition of cumyl hydroperoxide (CmO_2H) gives rise to an additional high-field shift (–536 ppm, one broad resonance) through the formation of the peroxido complex $[VO(O_2Cm)\text{-}L^A]$. Such a high-field shift is generally observed on exchanging OR^-, OH^- or O^{2-} for peroxide.[22,24] Since peroxide enhances binding of imidazole,[22] the coordination skeleton provided by the tetradentate ligand supposedly remains intact. The FAB mass spectrum of $[VO(OH)L^A]$ shows the mass peak at m/z = 433 with low intensity. The main peak, at m/z = 416, corresponds to the loss of an OH radical. For other typical peaks corresponding to the fragmentation of $[VO(L^A)]$ see Scheme 2. The V=O stretch at 924 cm^{-1} is comparatively low [commonly, ν(V=O) values are around 970 cm^{-1}] suggesting involvement of the oxido group in intermolecular hydrogen bonding or intramolecular "smearing" of the proton between OH and the doubly bonded O. A weak IR band at 506 cm^{-1} present in the complex but not in the ligand further supports the formulation $[VO(OH)L^A]$ with an oxido and hydroxido ligand, by analogy with, e.g., [VO(OH)-oxin] [oxin = 8-oxiquinolinate(1–)][25] and [VO(OH)Tp′] [Tp′ = tris(3,5-diisopropyl-1-pyrazolyl)borate(1–)].[26] Presumably, the OH ligand in our case originates from the hydrolysis of a $[VO(OiPr)L^A]$ intermediate in the presence of residual amounts of water.

The complex $[VO(H_2L^B)]$, with the preliminary formulation depicted in Scheme 1, forms on treating $[VO(OiPr)_3]$ with H_5L^B in polar solvents. The chemical shift $\delta(^{51}V)$ in

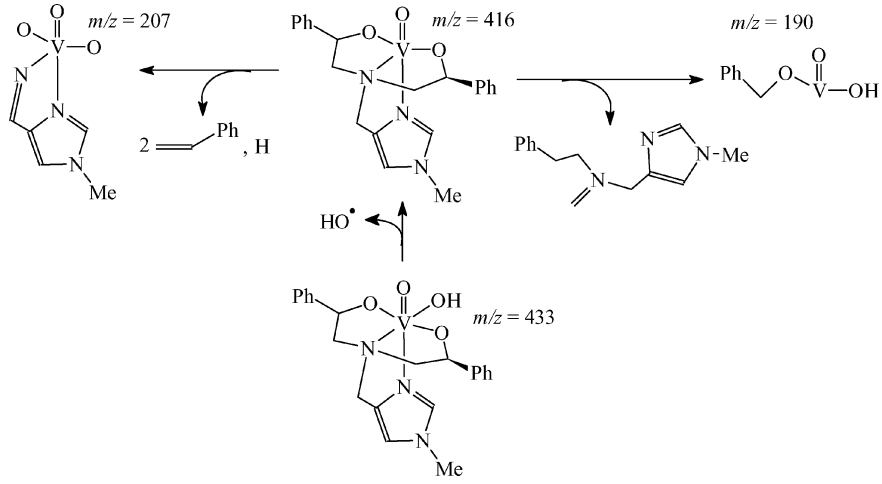

Scheme 2.

freshly prepared solutions in CD_3Cl is –411 ppm. After standing, the solutions turn green due to formation of an oxidovanadium(IV) complex, possibly of composition $[VO(H_3L^B)]$, the EPR parameters of which are $A_\perp = 68.0$, $A_\parallel = 172.0 \times 10^{-4}$ cm^{-1}; $g_\perp = 1.988$, $g_\parallel = 1.950$.

Reaction of H_4L^C with $[VO(OiPr)_3]$ in anhydrous ethanol under N_2 yields a red-brown solution and a light yellow precipitate. From the solution, yellow-green cubic crystals of the hexacoordinate complex $[VO(HL^C)]_{oct}\cdot C_2H_5OH$ were obtained in which all five ligand functions (the nitrogen, three deprotonated alcoholate groups and the protonated terminal propanol function) are coordinated to vanadium. From DMSO solutions of the precipitate, light yellow needle-like crystals of the pentacoordinate complex $[VO(HL^C)]_{tbp}$ were isolated. In $[VO(HL^C)]_{tbp}$, the terminal propanol −OH remains dangling. Apparently, the polarity of the solvent determines which of the structural variants is favoured. The ν(V=O) for both complexes, at 967 and 965 cm^{-1}, respectively, are in the expected range. The ^{51}V chemical shift for solutions of $[VO(HL^C)]_{oct}$ is –411 ppm in CD_3OD and –396 ppm in $[D_6]$DMSO. The respective value for $[VO(HL^C)]_{tbp}$ in $[D_6]$DMSO is –381 ppm. These similar chemical shifts suggest that the solution structures are about the same, and the rather low shielding suggests that the structure corresponds to an approximately ideal trigonal bipyramid in both cases. Trigonal-bipyramidal complexes of composition [VO(OMe)L], where L is the dianion of a tridentate aminoethanol, give rise to two signals in the ^{51}V NMR spectrum due to the presence of isomers with the oxido group in the equatorial and axial positions, respectively. An example is the distorted trigonal-bipyramidal (τ = 0.72) complex derived from H_2L = {HOCH(Ph)-CH_2}$_2$NCH$_2$CO(O*t*Bu), with $\delta(^{51}V)$ values of –449 and –470 ppm.[16] In solutions of $[VO(HL^C)]$, with the tetradentate ligand $(HL^C)^{3-}$ providing a rigid coordination environment, there is only one species present in which the oxido ligand is in the axial position, see $[VO(HL^C)]_{tbp}$ in Scheme 1. $[VO(HL^C)]_{oct}$ and $[VO(HL^C)]_{tbp}$ have been structurally characterised. The solid-state structures are shown in Figure 2. For selected structural parameters see Table 2. In both structures, the ligand is in the *R*,*R*,*S*-configuration (*S* configuration for C32).

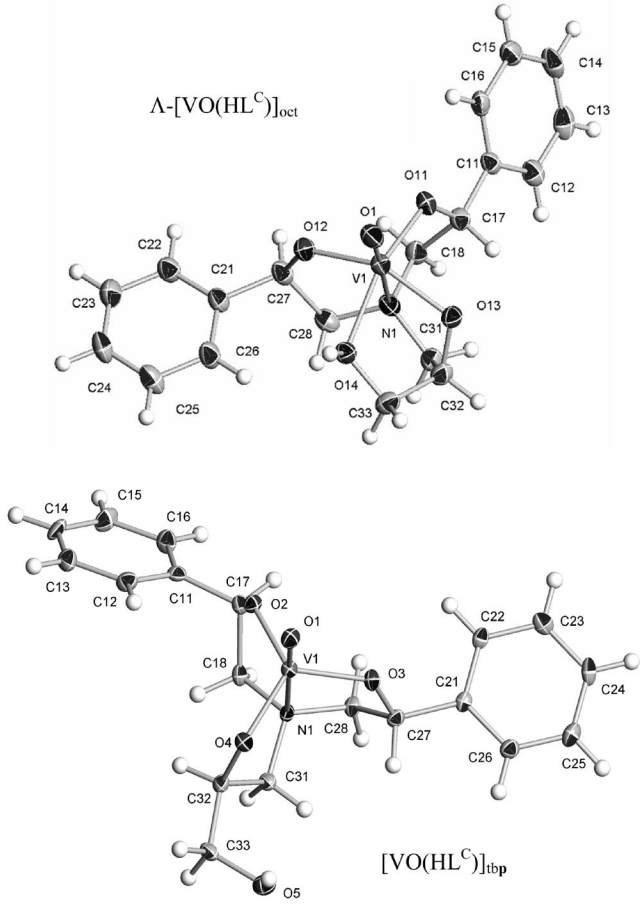

Figure 2. Structure representations of the octahedral and trigonal-bipyramidal complexes of composition $[VO(HL^C)]$.

In the case of $[VO(HL^C)]_{oct}\cdot C_2H_5OH$, there are two independent molecules in the asymmetric unit with very similar bonding characteristics. The terminal hydroxy group (O14)

Table 2. Selected bond lengths [Å] and angles [°] for $[VO(HL^C)]_{oct}\cdot C_2H_5OH$ and $[VO(HL^C)]_{tbp}$.

Λ-$[VO(HL^C)]_{oct}\cdot C_2H_5OH$[a]		$[VO(HL^C)]_{tbp}$	
V1–O1	1.6065(17)	V1–O1	1.6074(15)
V1–N1	2.297(2)	V1–N1	2.2987(17)
V1–O11	1.8236(17)	V1–O2	1.8183(16)
V1–O12	1.8423(18)	V1–O3	1.8024(15)
V1–O13	1.9324(18)	V1–O4	1.8097(16)
V1–O14	2.0753(19)	V1–O5	–
O1–V1–N1	178.15(9)	O1–V1–N1	179.74(10)
O11–V1–O12	102.39(8)	O2–V1–O3	115.38(8)
O11–V1–O13	89.97(8)	O2–V1–O4	117.73(8)
O11–V1–O14	158.38(9)	O2–V1–O5	–
O12–V1–O13	149.77(8)	O3–V1–O4	116.33(8)

[a] For one of the two molecules in the asymmetric unit.

in the propane side-chain gives rise to a comparatively long *d*(V–OH) = 2.075(2) Å. Together with the three hydroxido functions [*d*(V–O) = 1.823–1.932 Å], this hydroxy group forms the octahedral plane. The vanadium is only 0.041 Å displaced from this plane. One of the apical positions is occupied by the doubly bonded oxygen and the other by nitrogen at the rather long distance of 2.297(2) Å, a consequence of the trans influence by the oxido ligand. The two independent molecules are linked by rather short intermolecular hydrogen bonds between (OH)14···O23 (2.449) and O13···(HO)24. In addition, weak hydrogen bonds are present between the two ethanol molecules in the crystal (2.856 Å), and ethanol and O12 (2.840 Å). There are no distinct differences in bonding parameters between the free ligand H_4L^C and the coordinated ligand $(HL^C)^{3-}$, with the exception of the angles at C8/C18 and C33 which are narrower in the complex than in the free ligand. The chiral vanadium centre is in the anticlockwise (Λ) configuration.

The ligand arrangement in $[VO(HL^C)]_{tbp}$ is trigonal bipyramidal. The complex thus structurally resembles related vanadium complexes [VO(OR)L] containing tridentate aminodiethanolato ligands.[16–19] There are, however, also distinct differences: while, in the complexes [VO(OR)L], the doubly bonded oxido group is in the equatorial position in the crystalline solid state, it occupies an axial position in $[VO(HL^C)]_{tbp}$ as a consequence of steric demands imparted by the tetradentate ligand. This arrangement also implies an almost ideal trigonal-bipyramidal structure while, in [VO(OR)L] (H_2L = tridentate diethanolamine; R = Me or *i*Pr), there is always some distortion towards the square pyramid: τ parameters are commonly around 0.73 (τ = 1 for an ideal trigonal bipyramid, τ = 0 for an ideal square pyramid). As a consequence of the different geometries, most of the bond lengths and angles differ largely between $[VO(HL^C)]_{tbp}$ and $[VO(HL^C)]_{oct}$, see Table 2. In $[VO(HL^C)]_{tbp}$, the vanadium is 0.3439 Å above the trigonal plane formed by the three coordinating −O⁻ functions (O2, O3, O4). The dangling −OH is hydrogen bonded to the coordinated O2 of a neighbouring molecule and O2···(HO)5 = 2.851 Å.

Immobilisation on Merrifield and Barlos Resin

Merrifield and Barlos resins, copolymers based on styrene and (ca. 1% of) divinylbenzene contain a small percentage of *p*-(chloromethyl)phenyl (Merrifield) or 2-chlorotrityl chloride (Barlos) side chains. The resins, which are widely used in biochemical contexts, have been employed here to ascertain the integrity of the vanadium complexes which would be otherwise jeopardised by the presence of acidic groups such as in silica gels.[27] Tethering of an oxidovanadium complex to such a resin side-chain, subsequently symbolised by {}, was achieved with ligands H_5L^B, H_4L^C and $H_4L^{C'}$. Ligand H_3L^D, with a tertiary butyl group attached to the primary oxo group of the propanediol side-chain, models that structural unit of Barlos resin which anchors to the ligand system and demonstrates that the primary alcoholic group is the one which primarily reacts with the resin.

The procedure with the Merrifield resin was carried out in two steps: In step (i) the ligand H_4L^C, after conversion to $(H_3L^C)^-Na^+$ with NaH dissolved in THF, was anchored to the resin to yield the resin loaded with the ligand, $\{H_nL^C\}$ ($n \approx 3$; 0.27 mmol of ligand per g of resin). In step (ii) $\{H_nL^C\}$ was treated with a THF solution containing $[VO(O{i}Pr)_3]$ and stirred overnight, washed and dried to yield $\{[VO(L^C)]\}$ (0.22 mmol vanadium per g resin). The integrity of the complex was confirmed by IR and ^{51}V NMR spectroscopy. In the corresponding reaction with H_5L^B the original red-brown colour (indicative of $\{[V^VO(HL^B)]\}$) changed to green, suggesting the formation of $\{[V^{IV}O(H_2L^B)]\}$, Figure 3, i.e., a gradual reduction which has also been observed with the nonimmobilised complex (see above). EDX analysis revealed the presence of vanadium, Figure 3.

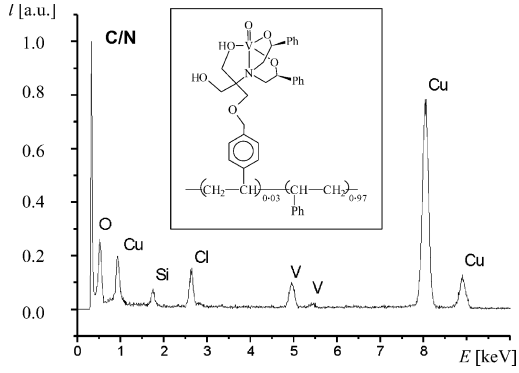

Figure 3. EDX spectrum of $[VO(O{i}Pr)H_2L^B]$ anchored to Merrifield resin (inset) showing the bands for C/N, O, Cl (residual chlorido groups of the resin) and V. The Cu peaks are due to the carrier material.

With Barlos resin, direct anchoring of the complex $[VO(HL^C)]$ was carried out in CH_2Cl_2 in the presence of Hünig's base to yield $\{[VO(L^C)]\}$ (0.34 mmol V per g resin). The corresponding reaction of Barlos resin with $[VOH_2L^B]$ in $DMSO/CH_2Cl_2$ resulted in the formation of $\{[VO(H_nL^B)]\}$ ($n \approx 1$; loading: 0.28 mmol V per g resin). The stability and integrity of the complex systems formed

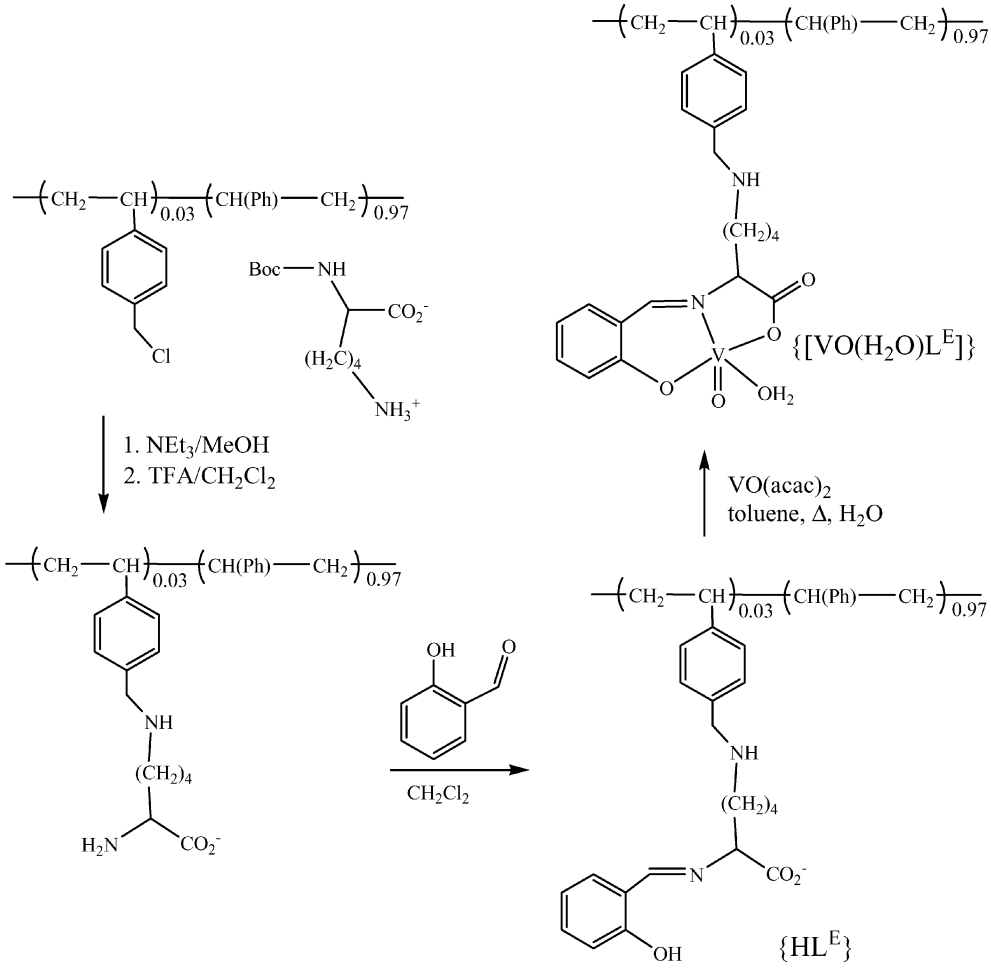

Scheme 3.

with [VO(H_nL^C)] were examined by ^{51}V NMR of mixtures of the complex with Hünig's base, and of the complex with trityl chloride plus Hünig's base (trityl chloride mimicking the functional unit of Barlos resin) in the same molar ratio as in the immobilisation reaction. The chemical shifts of these mixtures were identical within the limits of shift differences imparted by medium effects, Figure 4.

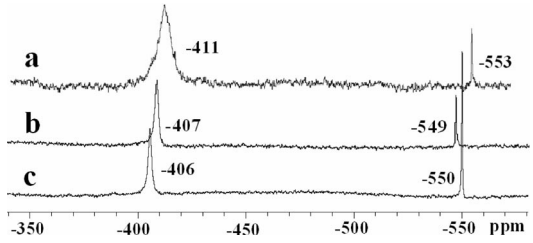

Figure 4. Comparison of the ^{51}V NMR spectra of (a) complex [VO(HL^C)], (b) [VO(HL^C)] + Hünig's base, and (c) [VO(HL^C)] + Hünig's base + trityl chloride. The minor signals at high field are due to an unidentified secondary product.

Generation of an oxidovanadium(IV) complex containing a Schiff base ligand (HL^E) tethered to a Merrifield resin was achieved as shown in Scheme 3. The resin was treated, in the presence of NEt_3, with Boc-protected lysine (Boc = *tert*-butyloxycarbonyl). After deprotection with trifluoroacetic acid (TFA), the lysine derivative of the resin was converted into the Schiff base derivative {HL^E} by condensation with salicylaldehyde. Further reaction with [VO(acac)$_2$] yielded the vanadium complex tethered to the Merrifield resin, {[VO(H_2O)L^E]}. Support for complexation comes from the disappearance, in the IR, of the phenol-OH band and the appearance of a new V=O stretching band at 985 cm^{-1}. Water as a neutral fifth ligand was added provisionally in order to satisfy the common pentacoordination found in oxidovanadium(IV) complexes of Schiff bases.[28]

Sulfoxygenation Reactions

The reactions have been carried out with thioanisol (MeSPh) using cumyl hydroperoxide (CmO_2H) as the oxidant, in chlorinated hydrocarbons. The overall reaction, Equation (2), corresponds to that for the sulfoxygenation of sulfides with H_2O_2 catalysed by vanadate-dependent haloperoxidases, see Eq. (1) in the Introduction. The precatalyst can either be the presynthesised complex itself, or the complex formed in situ from the precursor [VO(O*i*Pr)$_3$] and the

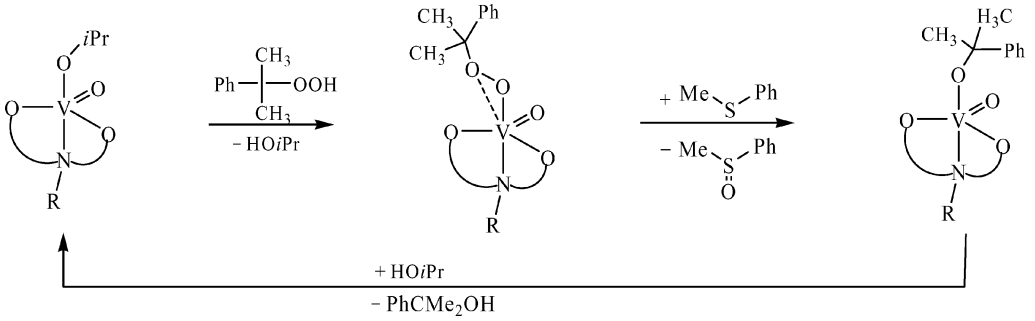

(2)

ligand. The active catalyst is a peroxido complex, containing the cumylperoxido ligand, viz. [VO(O$_2$Cm)L], possibly (as suggested by DFT calculations[16]) in the bent end-on coordination mode. The formation of the peroxido intermediate is visible by a colour change from yellow to orange and reflected in the ^{51}V NMR spectrum (see the above discussion for [VO(OH)L^A]). The substrate MeSPh nucleophilically attacks the activated peroxide to form the sulfoxide and, usually, a small percentage of sulfone as well. The vanadium complex is partly recovered in the form of [VO(OCm)L], again evidenced by ^{51}V NMR spectroscopy (–480 and –490 ppm in the case of L^A) and ^{1}H NMR spectroscopy (shift of the signal for the methyl protons from 1.59 ppm for CmO$_2$H to 1.56 ppm for CmOH). In addition, ligand-free peroxovanadates [HVO$_3$(O$_2$)]$^{2-}$ (–630 ppm) and [HVO$_2$(O$_2$)$_2$]$^{2-}$ (–683 ppm) are observed.

Selected results for the reactions catalysed under homogeneous conditions by [VO(OH)L^A], [VO(H$_2$L^B)] and [VO(HL^C)], and under heterogeneous conditions catalysed by the immobilised systems {[VO(H$_n$L^B)]}, {[VO(L^C)]} and {[VO(H$_2$O)L^E]} are summarised in Table 3. The time course for the reaction catalysed by [VO(OH)L^A] as followed by ^{1}H NMR spectroscopy is represented graphically in Figure 5 for 24 °C (left) and 0 °C (right).

Table 3. Collation of data for the catalytically conducted sulfoxygenation of thioanisol (methyl phenyl sulfide).[a]

Complex[b]	Conversion (%)	Time [h]	SO/SO$_2$[c]	*ee* (%), *isomer*
[VO(OH)L^A]	76	0.8	98:2	9, *R*
[VO(H$_2$L^B)]	89	3	97:3	2, *S*
H$_5$L^B + VO(O*i*Pr)$_3$	60	3	95:5	37, *R*
H$_5$L$^{B'}$ + VO(O*i*Pr)$_3$	89	3	95:5	7, *S*
[VO(HL^C)][d]	100	3	97:3	5, *S*
H$_4$L^C + VO(O*i*Pr)$_3$	100	3	98:2	6, *S*
{[VO(H$_2$L^B)]} (Barlos)	100	24	87:13	14, *S*
{[VO(HL^C)]} (Merrifield)	100	0.7	97:3	16, *S*
{[VO(HL$^{C'}$)]}[e] (Barlos)	100	24	98:2	19, *S*
{[VO(H$_2$O)L^E]}[f] (Merrifield)	95	6	98:2	16, *S*

[a] In $CHCl_3$ at 0 °C, *c*(sulfide) = 0.1 M, sulfide/oxidant/catalyst ratio = 1:1:0.1 (homogeneous) or 1:1:0.01 (heterogeneous systems). [b] Curly bracket {} represent complexes immobilised by tethering to the Merrifield or Barlos resin. [c] SO = sulfoxide, SO$_2$ = sulfone. [d] The trigonal-bipyramidal isomer has been employed in these experiments. [e] In CH_2Cl_2. [f] In toluene at room temp.; 1 mol-% catalyst.

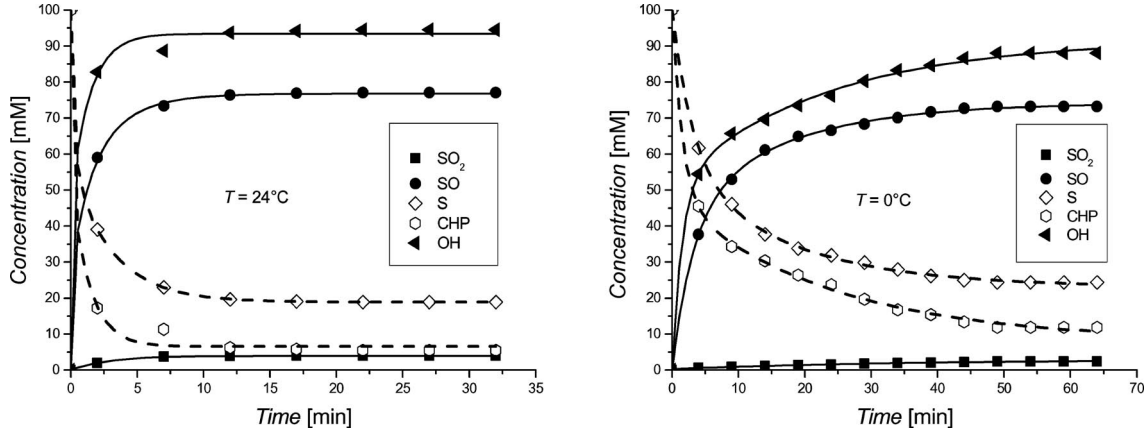

Figure 5. Time course of the oxygenation of thioanisol (S) by cumyl hydroperoxide (CHP), catalysed by [VO(OH)L^A] (cat). Conditions: *c*(S) = *c*(CHP) = 0.1 M, *c*(cat) = 0.01 M; solvent CH_2Cl_2; temperature 24 °C (left) and 0 °C (right). SO = sulfoxide, SO$_2$ = sulfone, OH = cumyl alcohol.

As evidenced by ^{51}V NMR spectroscopy in the homogeneous systems, the active species is also the peroxo intermediate where a mixture of the ligand and the vanadium precursor [VO(O*i*Pr)$_3$] is employed. Furthermore, most of the catalyst remains intact and the catalytic cycles can be repeated several times without substantial abatement in conversion rates. Particularly stable are the heterogeneous catalysts.

Conclusions

We have prepared chiral diethanolamines of the general composition {HOCH(Ph)CH$_2$}$_2$NR, where R is a functionalised (by imidazole or alcoholic groups) side-chain and employed these ligands in the synthesis of oxidovanadium(V) complexes with the vanadium centre in a trigonal-bipyramidal or octahedral environment. Interestingly, the complex [VO(HL^C)] (R = 1,2-hydroxypropyl) has been crystallised as a pentacoordinate, trigonal-bipyramidal and a hexacoordinate octahedral variant. The OH functionalisation in the side-chain R has been exploited for immobilising the complexes on Merrifield and Barlos resins. These complexes model the active centre of vanadate-dependent peroxidases from marine macro-algae and they also model the sulfoxygenation activity of these enzymes, i.e. the conversion of prochiral thioanisol to chiral sulfoxide plus some sulfone, with cumyl hydroperoxide as the oxidant, both in homogeneous catalysis (with the isolated complexes or the in situ systems, i.e. vanadium precursor + ligand) and in heterogeneous catalysis (with the immobilised complexes). The selectivity (ratio sulfoxide/sulfone), conversion rates and enantioselectivities (*ee*) vary greatly with the systems under investigation. Chiral inversion with respect to the catalysts which have been employed in the *R* configurations, occurs in most cases. The *ee* values are notoriously low: the best result, an *ee* = 37%, was obtained with the in situ system VO(O*i*Pr)$_3$ + H$_5$L^B [R = tris(hydroxymethyl)methyl]. The selectivities, 95–98% sulfoxide, are satisfactory throughout. The immobilised systems employed here are superior to those which have been obtained by anchoring vanadium complexes to silica gels and mesoporous silica gels, where (partial) decomposition and thus deactivation of the complex occurs.[27]

Experimental Section

General and Instrumental Methods: Standard chemicals were obtained from commercial sources and used without further purification. Silica gel for chromatography was purchased from Merck (silica gel 60, 0.040–0.063 mm). Solvents were dried according to standard methods and distilled under argon and the reactions carried out by employing Schlenk techniques. Elemental analyses: C,N,H,O rapid analyser (Heraeus and Carlo–Erba); EDX: SEM Hitachi-S2500 instrument, equipped with a Genesis system with sapphire Si(Li)-detector (EDAX/AMETEK Inc.); ICP-OES: SPECTRO CIROS CCD spectrometer. IR spectra: KBr mulls, Perkin–Elmer FTIR 1720 FT spectrometer; ATR-IR spectra were recorded on a Bruker VERTEX 70 FTIR spectrometer. NMR spectra: Varian Gemini 200 or Bruker Avance 400 with the usual instrument settings. ^{51}V chemical shifts are referenced to $VOCl_3$. FAB MS: VG-Analytical 70–250S; matrix: *m*-nitrobenzyl alcohol, xenon beam.

Single crystal X-ray measurements were carried out at 153(2) K according to the ω-scan method on a SMART Apex CCD (Bruker)

Table 4. Crystal data and details of the structure determination.

	H$_4$L^C	H$_3$L^D	Λ-[VO(*R*,*R*,S-HL^C)]$_{oct}$·C$_2$H$_5$OH	[VO(*R*,*R*,S-HL^C)]$_{tbp}$
Emperical formula	$C_{19}H_{25}NO_4$	$C_{38}H_{39}NO_4$	$C_{21}H_{28}NO_6V$	$C_{19}H_{22}NO_5V$
M [g mol^{-1}]	331.40	573.70	441.38	395.32
Crystal system	orthorhombic	orthorhombic	tetragonal	orthorhombic
Space group	$P2_12_12_1$	$P2_12_12_1$	$P4_1$	$P2_12_12_1$
a [Å]	9.3360(8)	7.2471(8)	11.5705(5)	7.7973(8)
b [Å]	10.7743(10)	17.8576(19)	11.5705(5)	11.9461(12)
c [Å]	17.3992(15)	23.712(3)	31.755(2)	18.8807(19)
V [Å^3]	1750.2(3)	3068.7(6)	4251.3(4)	1758.7(3)
Z	4	4	8	4
ρ(calcd.) [g cm^{-3}]	1.258	1.242	1.379	1.493
μ(Mo-K_α) [mm^{-1}]	0.088	0.080	0.503	0.595
F(000)	712	1224	1856	824
Crystal size [mm]	0.38 × 0.29 × 0.12	0.50 × 0.10 × 0.07	0.43 × 0.29 × 0.14	0.50 × 0.07 × 0.05
θ (min., max.) [°]	2.22, 27.50	2.82, 27.50	1.87, 27.50	2.02, 27.49
Index ranges	$-12 \le h \le 11$, $-13 \le k \le 13$, $-22 \le l \le 22$	$-9 \le h \le 9$, $-23 \le k \le 23$, $-30 \le l \le 30$	$-14 \le h \le 15$, $-15 \le k \le 15$, $-41 \le l \le 41$	$-10 \le h \le 10$, $-15 \le k \le 15$, $-24 \le l \le 24$
Total data / R(int.)	20789 / 0.0454	36989 / 0.1362	51404 / 0.0783	21132 / 0.0742
Data / restraints / parameters	2284 / 14 / 237	3985 / 0 / 391	9699 / 3 / 533	4018 / 1 / 239
Gof on F^2	0.997	0.803	0.754	0.876
R_1, wR_2 [$I > 2\sigma(I)$]	0.0398, 0.0923	0.0457, 0.0668	0.0404, 0.0486	0.0368, 0.0623
R_1, wR_2 (all data)	0.0504, 0.0963	0.1084, 0.0782	0.0695, 0.0526	0.0526, 0.0663
Flack parameter	[a]	[a]	–0.005(12)	0.01(2)
Max. / min. residual density [e Å^{-3}]	0.328 / –0.166	0.210 / –0.222	0.603 / –0.343	0.584 / –0.323

[a] The absolute structure could not be determined reliably because of the light atom composition. The configuration indicated for the ligands in the text is based on that found for the ligands in the complexes.

diffractometer equipped with a graphite monochromator and a Mo-K_α radiation source. Frames were read with the SAINT program, absorption corrections were carried out with SADABS. For the determination of the space group the program XPREP was employed, for the solution and refinement of the structures the program systems SHELXS-97 and SHELXL-97 were utilised. The following hydrogen atoms were found: H_4L^C: O3H, and N1H [H disordered between O3 and N1]; *d*[O3–H = 0.840(1), *d*(N1–H) = 0.880(1)], O4H, $[VO(HL^C)]_{oct}\cdot C_2H_5OH$: O14H, O24 H, $[VO(HL^C)]_{tbp}$: O5H. All other H atoms were calculated in ideal positions. Crystal data and details of the data collection and refinement are summarised in Table 4.

The sulfoxygenation reactions were carried out in chloroform, dichloromethane or toluene solution containing equimolar (0.1 M) amounts of thioanisol and cumyl hydroperoxide and 10 (homogeneous system) or 1 mol-% (resins) of the catalyst, at room temperature and/or 0 °C. The progress of the reaction over time was monitored by ^{1}H NMR spectroscopy (methyl protons of the reactants and reaction products). The enantiomeric excess was determined through the intensity ratio of the ^{1}H NMR signals of the methyl protons of the sulfoxide which split into two components by formation of two diastereomeric adducts (*R*,*R* and *R*,*S*) on addition of pirkle alcohol, *R*-(–)-1-(9-anthranyl)-2,2,2-trifluoroethanol.

CCDC-667532 (for H_4L^C), -692716 (for H_3L^D), -669382 (for Λ-$[VO(R,R,S\text{-}HL^C)]_{oct}\cdot C_2H_5OH$) and -691872 (for $[VO(R,R,S\text{-}HL^C)]_{tbp}$) contain the supplementary crystallographic data for this paper. These data can be obtained free of charge from The Cambridge Crystallographic Data Centre via www.ccdc.cam.ac.uk/data_request/cif.

Preparation of Ligands and Complexes

***N*,*N*-Bis(2-hydroxyphenylethyl)-*N*-(1-methyl-1*H*-imidazol-4-yl)-methylamine (H_2L^A):** *R*-Styrene oxide (2.047 mL, 17.76 mmol) dissolved in absolute *tert*-butyl methyl ether (BME) (15 mL) were treated, under reflux conditions, over 3 h with (1-methyl-1*H*-imidazol-4-yl)methylamine (987 mg, 8.9 mmol) dispensed from a dropping funnel. The dropping funnel was rinsed twice with BME (25 mL) and the combined solutions heated to reflux until complete conversion of the epoxide (5 d). The solvent was removed in vacuo, the orange-yellow residue (3.04 g) dissolved in CH_2Cl_2/2-propanol (10:1) and chromatographed on silica gel (450 g, column diameter 8 cm). The fraction containing H_2L^A was evaporated to dryness in vacuo at 65 °C to yield 1.29 g (41%) of yellowish, oily H_2L^A. $C_{21}H_{25}N_3O_2$ (351.45): calcd. C 71.79, H 7.12, N 11.97; found C 71.53, H 7.13, N 11.57. IR (KBr): $\tilde{\nu}$ = 3435 (*ν*, OH), 2932 (and 2886 (*ν*, CH_2)), 2828 (R_2N–CH_2), 1631 (C=C), 1510 (C=N), 1451 (*δ*, CH_3), 1329 (*δ*, OH), 1094 (*ν*, CO) cm^{-1}. ^{1}H NMR ([D$_6$]acetone, number of protons, *assignments printed in italics*, cf. Scheme 4), *δ* = 7.44 (s, 1 H, *j*), 7.40 (d, 4 H, *c*), 7.29 (t, 4 H, *b*), 7.20 (t, 2 H, *a*), 6.95 (s, 1 H, *h*), 4.87 (dd, 3.3 and 9.9, 2 H, *d*), 3.91 (d, 14.9, 1 H, *f*), 3.76 (d, 14.9, 1 H, *g*), 3.63 (s, 3 H, *i*), 2.70 (dd, 14.1, 4 H, *e* and *e*′) ppm. ^{13}C NMR ([D$_6$]acetone, *assignments printed in italics*, cf. Scheme 4): *δ* = 144.89 (*4*), 140.05 (*8*), 138.68 (*11*), 128.86 (*2*), 127.68 (*1*), 126.95 (*3*), 119.66 (*9*), 71.11 (*5*), 64.42 (*6*), 52.29 (*7*), 33.55 (*10*) ppm. FAB-MS: *m*/*z* = 352.3 [M$^+$ + 1, 88], 244.2 (M$^+$ – $PhCH_2OH$, 100). $C_{21}H_{25}N_3O_2$ (351.45): calcd. C 71.79, H 7.12, N 11.97; found C 71.53, H 7.13, N 11.57. FAB MS: *m*/*z* = (assignment): 352 (M +1), 244 (M + 1 – $C_6H_5CH_2OH$).

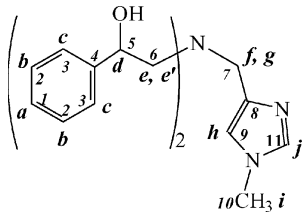

Scheme 4.

***N*,*N*-Bis(2-hydroxy-2-phenylethyl)-*N*-[tris(hydroxymethyl)methyl]-amine (H_5L^B), and *N*-(2-Hydroxy-2-phenylethyl)-*N*-(2-hydroxy-1-phenylethyl)-*N*-[tris(hydroxymethyl)methyl]amine ($H_5L^{B'}$):** Styrene oxide (1.43 mL, 12.5 mmol) and tris(hydroxy)methylamine (758 mg, 6.3 mmol) dissolved in 2-propanol (15 mL) were heated to reflux for 4 d and the product purified by column chromatography on silica gel using hexane/ethyl acetate followed by ethyl acetate/ethanol with gradually increasing polarity. Both products thus isolated, H_5L^B (52% yield) and $H_5L^{B'}$ (22% yield) are colourless, sticky, gel-like substances. $C_{20}H_{27}NO_5$ (361.44): calcd. C 66.46, H 7.53, N 3.88; found for H_5L^B C 65.82, H 7.49, N 3.41. ^{1}H NMR ([D$_6$]acetone, cf. Scheme 5)]: *R*,*R*-H_5L^B: *δ* = 7.36 (m, 10, *Ph*), 4.94 (AB*X*) and 2.91 + 2.78 [(*AB*X), 6 H, *2 and 4*], 3.75 (s, 6 H, *3*) ppm. *R*,*R*-$H_5L^{B'}$: *δ* = 7.35 (m, 10, *Ph*), 4.80 (AB*X*) and 2.91 + 2.78 (*AB*X) (3 H, *2 and 4*), 4.15 (AB*X*) and 3.58 + 3.44 (*AB*X) (3 H, *2′ and 4′*), 3.55 (s, 6 H, *3*) ppm. ^{13}C NMR ([D$_6$]acetone, *assignments printed in italics*, cf. Scheme 5): *R*,*R*-H_5L^B: *δ* = 72.4 (*2*), 64.4 [*C*$(CH_2OH)_3$], 63.9 (*3*), 58.5 (*4*) ppm. *R*,*R*-$H_5L^{B'}$: *δ* = 73.5 (*2*), 67.1 (*2′*), 64.4 [*C*$(CH_2OH)_3$], 62.6 (*4′*), 62.0 (*3*), 52.4 (*4*) ppm.

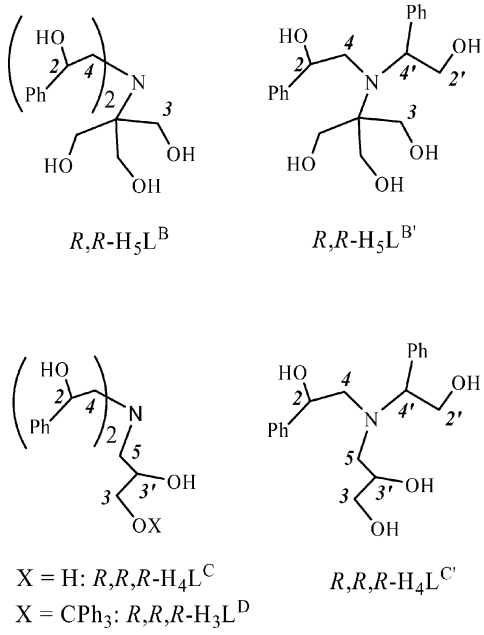

Scheme 5.

***N*,*N*-Bis(2-hydroxy-2-phenylethyl)-*N*-(2,3-dihydroxypropyl)amine (*R*,*R*,*S*-H_4L^C) and *N*-(2-Hydroxy-2-phenylethyl)-*N*-(2-hydroxy-1-phenylethyl)-*N*-(2,3-dihydroxypropyl)amine ($H_4L^{C'}$):** R-Styrene oxide (1.43 mL, 12.5 mmol) and 3-amino-1,2-propanediol (0.487 mL, 6.3 mmol) were dissolved in 2-propanol (10 mL) in a small flask and heated to reflux for 6 d. By purification using chromatography on silica gel as described for H_5L^B, two fractions were isolated. The first fraction, after evaporation, yielded a colourless white solid of *R*,*R*,*S*-H_4L^C (59% of the overall amount of product formed). The second fraction was a colourless liquid consisting of a mixture of the isomers $H_4L^{C'}$ (32%). $C_{19}H_{25}NO_4$ (331.40): calcd. C 68.80, H 7.54, N 4.22; found for H_4L^C C 68.24, H 7.58, N 4.10. ^{1}H NMR

(CD_3OH, number of protons, *assignments printed in italics*, cf. Scheme 5): *R,R,S*-H_4L^C: δ = 7.30 (10, *Ph*), 4.82 (AB*X*) and 2.80 + 2.72 (*AB*X) (6 H, *2 and 4*), 3.78 (m, 1 H, *3′*), 3.53 (m, 2 H, *3*), 2.90 and 2.73 (m, 6 H, *4 and 5*) ppm. *R,R,S*-$H_4L^{C'}$: δ = 7.33 (m, 10 H, *Phc*), 4.82 (AB*X*) and 2.81 + 2.63 (*AB*X) (3 H, *2 and 4*), 3.98 (AB*X*) and 4.01 + 3.78 (*AB*X) (3 H, *2′ and 4′*), 3.70 (1 H, *3′*), 3.39 and 3.47 (m, 2 H, *3*), 2.80 and 2.53 (m, 2 H, *5*) ppm. ^{13}C NMR (CD_3OD, *assignments printed in italics*, cf. Scheme 5): H_4L^C: δ = 70.8 (*2*), 68.1 (*3′*), 64.01 (*3*), 63.9 (*3*), 58.7 (*5*) ppm. $H_4L^{C'}$: δ = 69.1 (*2*), 68.0 (*3′*), 66.2 (*4′*), 62.1 (*3*), 60.0 (*4*), 52.5 (*5*) ppm.

***N*,*N*-Bis(2-hydroxy-2-phenylethyl)-*N*-(2-hydroxy-3-triphenylmethoxypropyl)amine (*R*,*R*,*R*-H_4L^D):** H_4L^C (100.9 mg, 0.31 mmol) was dissolved in CH_2Cl_2 (4 mL) and treated with trityl chloride (85.3 mg, 0.31 mmol) and Hünig's base (0.101 mL, 0.58 mmol). The reaction mixture was stirred for 24 h, the solvent evaporated and the residue redissolved in anhydrous acetone. Slow evaporation within a few days afforded needle-shaped colourless crystals in 98% yield. ^1H NMR ($CDCl_3$, number of protons, *assignments printed in italics*, cf. Scheme 5): δ = 7.33 (m, 25 H, *Ph*), 4.70 (AB*X*) and 2.80 + 2.76 (*AB*X) (6 H, *2 and 4*), 3.92 (m, 1 H, *3′*), 3.20 (m, 2 H, *3*), 2.60 and 2.49 (m, 2 H, *5*) ppm. ^{13}C NMR ($CDCl_3$, *assignments printed in italics*, cf. Scheme 5): δ = 87 (*C*Ph_3), 71 (*2*), 70 (*3*), 68 (*5*), 63 (*4*), 58 (*3′*) ppm.

[VO(OH)L^A]: H_2L^A (78.6 mg, 0.224 mmol) dissolved in THF (3 mL) was treated with [VO(O*i*Pr)$_3$] (54.6 mg, 52.7 μL, 0.224 mmol) and stirred for 12 h. From the yellow-orange solution, the solvent was removed in vacuo. The residue was redissolved in [D_8]THF and stored at –20 °C for 24 h. The red-brown precipitate of [VO(OH)(L^A)] was recovered and dried. Yield 29.2 mg (31.3%). IR (KBr): $\tilde{\nu}$ = 2926 and 2853 (CH_2), 1451 (δ, CH_3), 1093 (CO), 924 (V=O), 506 (VOH) cm^{-1}. ^{51}V NMR (CD_2Cl_2), δ (integral) = –459.3 (1.0), –501.2 (0.68) ppm. FAB-MS, *m/z* [assignment (cf. also Scheme 2), relative intensity]: 433 [M^+, 6], 416 (M^+ – OH, 94), 207.0 [M^+ – 1 – (2 styrenes), 100], 190.0 [(M^+ – 1) – 1-*N*-methylene-*N*-(1-methylimidazolyl)ethaneammonium, 54]. $C_{21}H_{23}N_3O_3V$ (433.37): calcd. C 58.20, H 5.58, N 9.70, V 11.76; found C 57.71, H 5.52, N 9.54, V 12.14.

In the following descriptions in curly brackets { } symbolise the resin matrix. All preparations directed towards the vanadium complexes were conducted under N_2.

[VO(H_2L^B)]: H_5L^B (151 mg, 0.42 mmol) dissolved 2-propanol (2 mL) were treated dropwise whilst stirring with [VO(O*i*Pr)$_3$] (0.11 mL, 0.42 mmol) dissolved in 2-propanol (4.5 mL) to produce an orange solution which, over the course of time, became dark orange with simultaneous formation of a yellow precipitate. The precipitate was filtered after 10 h, washed with THF and dried in vacuo. Freshly prepared solutions in $CDCl_3$ show a single resonance in the ^{51}V NMR spectrum at δ = –411 ppm and a ν(V=O) of 965 cm^{-1}. On storage the solutions turn green, a change which is accompanied by the disappearance of the NMR signal and appearance of an EPR signal typical of VO^{2+} (see Results and Discussion for data).

Immobilisation on Merrifield and Barlos Resin, {[VO(H_nL^B)]}: Merrifield resin (0.5 g) was macerated in *p*-xylene (10 mL) for 24 h at room temp. and treated with H_5L^B (152 mg, 0.42 mmol) dissolved in a mixture of *p*-xylene (2 mL) and DMF (1 mL). This mixture was stirred while Hünig's base (0.14 mL, 0.80 mmol) was added to the system. The mixture was then heated to reflux, under N_2, for 72 h, cooled to room temp. and washed three times with ethanol and finally with water, carbonate buffer then and ethanol/CH_2Cl_2 (1:1). The resin loaded with the ligand, {H_nL^B}, was pumped dry and kept under N_2. Loading rate according to elemental nitrogen analysis: 0.27 mmol of ligand per g of resin. {H_nL^B} (165 mg) was suspended in anhydrous $CHCl_3$ containing [VO(O*i*Pr)$_3$] (9.5 μL) (corresponding to a ligand/V ratio of 1:1). The vanadium-loaded, initially red-brown resin, {[VO(H_nL^B)]}, changed colour to green on stirring overnight. It was filtered off, washed with $CHCl_3$, THF and again with $CHCl_3$, then dried. See Figure 2 in the Discussion section for the EDX analysis.

To a suspension of [VO(H_2L^B)] (96.6 mg, 0.23 mmol) in CH_2Cl_2 (1 mL) was added DMSO (0.4 mL) which resulted in the formation of a clear solution. To this solution was added Barlos resin (101.8 mg) and Hünig's base (0.16 mL, 0.92 mmol). After 24 h of stirring, the loaded resin, {[VO(H_nL^B)]}, was filtered, washed six times with anhydrous CH_2Cl_2 then dried in vacuo. Vanadium analysis: found 1.74%, corresponding to a loading of 0.28 mmol of V per g of the resin. IR (KBr): $\tilde{\nu}$ = 978 (V=O) cm^{-1}.

Λ-[VO(*R*,*R*,*S*-HL^C)]$_{oct}$, [VO(*R*,*R*,*S*-HL^C)]$_{tbp}$ and Immobilisation on Merrifield and Barlos Resin, {[VO(L^C)]}: H_4L^C (350 mg, 1.06 mmol) was dissolved in anhydrous ethanol (2 mL) and treated dropwise and with stirring with an ethanol solution (10 mL) containing [VO(O*i*Pr)$_3$] (0.25 mL, 1.16 mmol). The initially red-brown solution turned orange and a yellow precipitate finally formed which was filtered off. From the filtrate, kept at –20 °C for a couple of days, yellow-green cubic crystals of [VO(HL^C)]$_{oct}$·C_2H_5OH were obtained. If THF is used instead of ethanol, fine needle-like crystals are obtained. IR (KBr): $\tilde{\nu}$ = 967 (V=O) cm^{-1}. ^{51}V NMR ([D_6]-DMSO): δ = –396 ppm.

The precipitate was dissolved in DMSO. From this solution, kept at room temperature for two weeks, light yellow needles of [VO(HL^C)]$_{tbp}$ could be isolated. IR (KBr): $\tilde{\nu}$ = 965 (V=O) cm^{-1}. ^{51}V NMR ([D_6]DMSO): δ = –381 ppm.

Immobilisation on Merrifield Resin: NaH (65 mg, 1.63 mmol, 60% in paraffin) was washed several times with anhydrous hexane to remove the paraffin and dried in vacuo. To this NaH was added H_4L^C (530 mg, 1.60 mmol) dissolved in THF (6 mL). The slurry was stirred for 4 h at room temp. and treated with Merrifield resin (360 mg, 0.7 mmol Cl g^{-1}) previously swelled in THF (6 mL) for 6 h. After stirring overnight, the slurry was washed with water, ethanol and THF (three times each) and dried in vacuo. Elemental analysis: found N 0.37, C 88.51, H 7.65. A loading of 0.27 mmol H_nL^C per g of resin was established from the nitrogen analysis. IR confirmed the integrity of the ligand, e.g. by the presence of the characteristic ν(CO) at 1065 cm^{-1}. To the immobilised {H_nL^C} (253 mg) was added [VO(O*i*Pr)$_3$] (0.075 mL, 0.32 mmol; 1.2 molar excess with respect to the ligand) and the mixture stirred overnight at room temp. The brown coloured, loaded resin was than filtered off and washed five times with THF, ethanol and finally acetone then dried in vacuo. Vanadium analysis of {[VO(L^C)]}: found 1.12%, corresponding to a loading of 0.22 mmol of V per g of resin. IR (KBr): $\tilde{\nu}$ = 975 (br, V=O) cm^{-1}.

Immobilisation on Barlos Resin: Resin (100.5 mg, 0.10 mmol based on 1.0 mmol g^{-1}) and [VO(HL^C)]$_{oct}$ (79.6 mg, 0.20 mmol) were suspended in anhydrous CH_2Cl_2 (1.0 mL) and treated with Hünig's base (0.14 mL, 0.81 mmol) resulting in complete dissolution of the complex. After 24 h of stirring, the loaded resin was filtered, washed six times with CH_2Cl_2 and pumped dry. Vanadium analysis of {[VO(L^C)]}: found 1.74%, corresponding to a loading of 0.34 mmol of V per g of resin.

{[VO(H_2O)L^E]} ≡ [VO(H_2O)L^E] Immobilised to Merrifield Resin: (cf. also Scheme 3 in the Results and Discussion section.) α-Boc-ε-Z-lysine (2 g, 3.5 mmol) was converted into α-Boc-lysine in methanol/$CHCl_3$, (100 mL, 95:5) in the presence of freshly prepared pal-

ladium black (200 mg) by continuous stirring for 4 h under H_2. The catalyst was filtered, washed with methanol/CH_2Cl_2 and the filtrate evaporated to dryness. 700 mg (47% yield) of α-Boc-lysine was thus obtained. α-Boc-lysine (170 mg, 0.4 mmol) was dissolved in methanol (10 mL) and treated with NEt_3 (40 mg, 0.4 mmol). To this solution was added, under N_2, a methanolic suspension (10 mL) of Merrifield resin (520 mg, 0.4 mmol) pretreated with NEt_3 (134 mg, 1.33 mmol). The successful anchoring was monitored by, inter alia, the disappearance of the C–Cl stretch (870 cm^{-1}). The product {Boc-lysine$^-$}[Et_3NH]$^+$ thus obtained was suspended in CH_2Cl_2 (10 mL). Deprotection (removal of the Boc group) was achieved by addition of trifluoroacetic acid (22.4 g, 0.2 mol, TFA), followed by treatment with NEt_3 (19.7 g, 0.2 mol). Deprotection was indicated by the disappearance of the amide stretching mode at 1631 cm^{-1}. To this solution, containing {lysine$^-$}[Et_3NH]$^+$, was added salicylaldehyde (sal, 97.6 mg, 0.8 mmol) dissolved in CH_2Cl_2 (10 mL) and the solution was heated to reflux for 2 h. The polymer {sallys$^-$}[Et_3NH]$^+$ ≡ {HL^E}[Et_3NH] resulting from this condensation reaction was filtered, washed several times with CH_2Cl_2 and dried under vacuum. The product contained residual amounts of [Et_3HN]TFA (evidenced by the C–F stretch at 1244 cm^{-1}). {HL^E}[Et_3NH] (475 mg) was added with stirring and in an N_2 atmosphere to a solution of [VO(acac)$_2$] (96 mg, 0.36 mmol) dissolved in toluene (20 mL). The reaction mixture was heated to reflux for 24 h and the supported complex {[$VO(H_2O)L^E$]} isolated by filtration, washed with toluene and water under N_2 and dried in vacuo. EDX analysis showed the presence of vanadium and fluorine. The latter can be removed by repeated washings with water.

Acknowledgments

This work was supported by the Deutsche Forschungsgemeinschaft (DFG) (grant RE 431/20). We acknowledge assistance in the XDS (Prof. U. Behrens, University of Hamburg) and EDX analyses (Dr. K. Hofmann, Technical University of Darmstadt).

[1] C. H. Senanayake, D. Krishnamurthy, Z.-H. Lu, Z. Han, I. Gallou, *Aldrichimica Acta* **2005**, *38*, 93–103.
[2] L. Y. Juliette, M. R. Hyman, D. J. Arp, *Appl. Environ. Microbiol.* **1993**, *53*, 3718–3727.
[3] C. Colonna, N. Gaggero, P. Pasta, G. Ottolina, *Chem. Commun.* **1996**, 2303–2307.
[4] a) M. Horinouchi, T. Yoshida, H. Nojiri, H. Yamane, T. Omori, *Biotechnol. Lett.* **1999**, *21*, 929–933; b) D. R. Boyd, N. D. Sharma, S. A. Haughey, J. F. Malone, B. T. McMurray, G. N. Sheldrake, C. C. R. Allen, H. Dalton, *Chem. Commun.* **1996**, 2363–2364.
[5] a) M. A. Andersson, S. G. Allenmark, *Tetrahedron* **1998**, *54*, 15293–15304; b) M. A. Andersson, A. Willetts, S. Allenmark, *J. Org. Chem.* **1997**, *62*, 8455–8458.
[6] a) H. B. ten Brink, H. E. Schoemaker, H. van Lingen, R. Wever, *Tetrahedron: Asymmetry* **1999**, *10*, 4563–4572; b) H. B. ten Brink, H. E. Schoemaker, R. Wever, *Eur. J. Biochem.* **2001**, *268*, 132–138.
[7] M. Weyand, H. J. Hecht, M. Kieß, M.-F. Liaud, H. Vilter, D. Schomburg, *J. Mol. Biol.* **1999**, *293*, 595–611.
[8] D. Rehder, *Bioinorganic Vanadium Chemistry*, Wiley, Chichester, **2008**, ch. 4.3.2.
[9] D. Balcells, F. Maseras, A. Lledós, *J. Org. Chem.* **2003**, *68*, 4265–4274.
[10] K. Nakajima, K. Kojima, J. Fujita, *Bull. Chem. Soc. Jpn.* **1990**, *63*, 2620–2630.
[11] C. Ohta, H. Shimizu, A. Kondo, T. Katsuki, *Synlett* **2002**, 161–163.
[12] a) C. Bolm, F. Bienewald, *Angew. Chem. Int. Ed. Engl.* **1996**, *34*, 2640–2642; b) C. Bolm, *Coord. Chem. Rev.* **2003**, *237*, 245–256.
[13] S. A. Blum, R. G. Bergman, J. A. Ellmann, *J. Org. Chem.* **2003**, *68*, 150–155.
[14] W. Adam, D. Golsch, J. Sundermeyer, G. Wahl, *Chem. Ber.* **1996**, *129*, 1177–1182.
[15] T. S. Smith II, V. L. Pecoraro, *Inorg. Chem.* **2002**, *41*, 6754–6760.
[16] C. Wikete, P. Wu, G. Zampella, L. De Gioia, G. Licini, D. Rehder, *Inorg. Chem.* **2007**, *46*, 196–207.
[17] D. Rehder, G. Santoni, G. M. Licini, C. Schulzke, B. Meier, *Coord. Chem. Rev.* **2003**, *237*, 53–63.
[18] G. Santoni, G. Licini, D. Rehder, *Chem. Eur. J.* **2003**, *9*, 4700–4708.
[19] a) P. Wu, G. Santoni, C. Wikete, D. Rehder, *ACS symposium series 974* (Vanadium), **2007**, 61–69; b) P. Wu, G. Santoni, M. Fröba, D. Rehder, *Chem. Biodivers.*, in the press.
[20] K. Fukui, H. Ohya-Nishiguchi, H. Kamada, *Inorg. Chem.* **1998**, *37*, 2326–2327.
[21] V. Vergopoulos, W. Priebsch, M. Fritzsche, D. Rehder, *Inorg. Chem.* **1993**, *32*, 1844–1849.
[22] H. Schmidt, I. Andersson, D. Rehder, L. Pettersson, *Chem. Eur. J.* **2001**, *7*, 251–257.
[23] D. Rehder, C. Weidemann, A. Duch, W. Priebsch, *Inorg. Chem.* **1988**, *27*, 584–587.
[24] A. González Baró, I. Andersson, L. Pettersson, A. Gorzsás, *Dalton Trans.* **2008**, 1095–1102.
[25] L. W. Amos, D. T. Sawyer, *Inorg. Chem.* **1974**, *13*, 78–83.
[26] M. Kosugi, S. Hickichi, M. Akita, Y. Moro-oka, *Inorg. Chem.* **1999**, *38*, 2567–2578.
[27] P. Wu, G. Santoni, M. Fröba, D. Rehder, *Chem. Biodiv.* **2008**, in press.
[28] D. Rehder, C. Schulzke, H. Dau, C. Meinke, J. Hanns, M. Epple, *J. Inorg. Biochem.* **2000**, *80*, 115–121.

Received: August 1, 2008
Published Online: October 17, 2008

